Large Area Thermal and Fast Neutron Detector Based on Bragg-Peak Detection

Final Report

Georgia Institute of Technology

Nolan E. Hertel

October 7, 2009

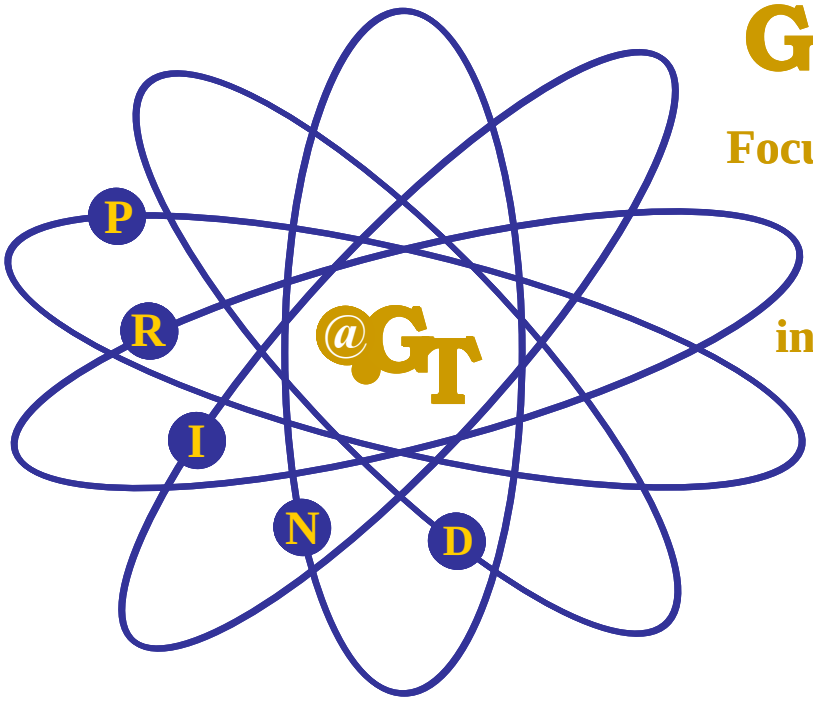

GaTech

Focused Research Program

Pioneer Research in Nuclear Detection

Table of Contents

Table of Figures

Introduction

There is an ongoing effort to produce a near term replacement for ^{3}He tubes. These thermal neutron detectors were a staple of neutron detection due to their large size, high efficiency and neutron-gamma discrimination capabilities. The researchers at PNNL have envisioned a system which utilizes lithium fluoride (LiF) grains surrounded by scintillator materials as a possible replacement for ^{3}He tubes. In support of the DOE/NA-22 Scintillator Bead project, Georgia Tech has collaborated with PNNL to show feasibility of using micron-sized scintillation coatings with micron-sized ^{6}LiF beads for the detection of thermal neutrons in optical fiber geometries. Georgia Tech's efforts have included optical modeling of the fibers, neutron detector modeling, and the investigation of various coating techniques. Georgia Tech has also investigated the potential testing of lithium fluoride grains and coatings should they come available. A description of typical testing configurations will be described later in the document.

Fiber Optic Modeling

Theory

The primary approach used for the optical fiber design problem is classical waveguide theory with a three layer cylindrical model: core (layer I), cladding (layer II), and the outermost medium (layer III), which extends to infinity as shown in Figure 1. The theory behind the infinite cylindrical waveguide is well known. By assuming a particular functional form with unknown coefficients for the coupled E_z and H_z field components in each region, all the other field components can be calculated.

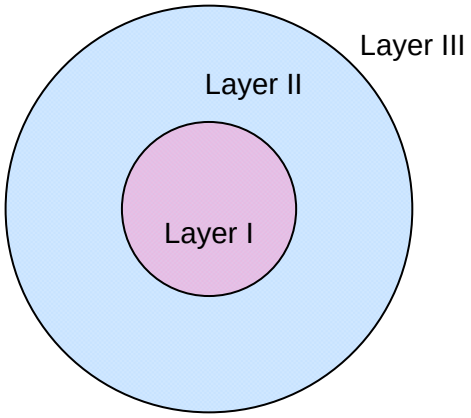

Figure 1. Assumed geometry of problem. The z-direction is the direction of propagation (out-of-plane direction).

In layer I,

$$E_z = A^I \frac{I_\nu(k_t^I \rho)}{I_\nu(k_t^I a)} \cos \nu\phi e^{-ik_z z} \qquad (1)$$

$$H_z = B^I \frac{I_\nu(k_t^I \rho)}{I_\nu(k_t^I a)} \sin \nu\phi e^{-ik_z z} \quad (2)$$

In layer II,

$$E_z = (A_1^{II} \frac{I_\nu(k_t^{II} \rho)}{I_\nu(k_t^{II} a)} + A_2^{II} \frac{K_\nu(k_t^{II} \rho)}{K_\nu(k_t^{II} a)}) \cos \nu\phi e^{-ik_z z} \quad (3)$$

$$H_z = (B_1^{II} \frac{I_\nu(k_t^{II} \rho)}{I_\nu(k_t^{II} a)} + B_2^{II} \frac{K_\nu(k_t^{II} \rho)}{K_\nu(k_t^{II} a)}) \sin \nu\phi e^{-ik_z z} \quad (4)$$

In layer III,

$$E_z = A^{III} \frac{K_\nu(k_t^{III} \rho)}{K_\nu(k_t^{III}(a+t))} \cos \nu\phi e^{-ik_z z} \quad (5)$$

$$H_z = B^{III} \frac{K_\nu(k_t^{III} \rho)}{K_\nu(k_t^{III}(a+t))} \sin \nu\phi e^{-ik_z z} \quad (6)$$

In the above equations, the A's and B's are the unknown coefficients of the Bessel waves in each layer, k_t = sqrt($k_z^2 - k^2$) is the transverse component of the wavevector, k_z is the out-of-plane component of the wavevector, k is the wavenumber in each dielectric medium, k_0 is the wavenumber in air, a is the radius of layer I (the core), and t is the thickness of layer II. $I_v()$ and $K_v()$ are the modified Bessel and modified Neumann functions, respectively. From the above formulations, the fields E_ρ, H_ρ, E_ϕ, and H_ϕ are calculated in each region using Maxwell's equations. The unknown A and B coefficients are obtained by matching the tangential field components at the cylindrical boundaries between each region. This results in an 8 × 8 matrix. The dispersion equation is obtained by setting the determinant of the matrix equal to zero. In our implementation, Newton's method is used to solve the dispersion equation. Any of these layers can be lossy, which allows for the modeling of metallic layers.

The above approach has been validated by testing 2-layer fiber problems against results obtained from Balanis [1]. In addition to the above approach, there are also finite element frequency domain electromagnetic codes at our disposal for problems with more than 3 layers. These include an in-house 2D FEM code and Ansoft HFSS.

Waveguide design considerations

- The proposed scintillator material, ZnS:Ag, emits at 450 nm (according to Saint-Gobain Crystals website).
- It would be advantageous to make the core as 'thin' as possible without making the fiber too fragile. This is because we would like to force the optical mode into the cladding to overlap with the scintillator material.
- A typical single-mode fiber for carrying infrared wavelengths is composed of silica with an 8 micrometer diameter core. We're operating at a much shorter wavelength, so we would not

expect an 8 micrometer diameter core to be single-mode in our case. I assume that making the core thinner than this will make the fiber too fragile, so the core has been set to be 8 micrometer diameter silica for the initial simulations.

- The ^{6}LiF particles are 10 micrometers in diameter. The entire fiber cladding has been assumed to be composed of ^{6}LiF for simplicity in modeling. The particles will be coated with ZnS:Ag, but since the thickness of that layer is unknown, it is neglected for now.
- The relatively large index contrast between the silica core (n = 1.47 at 450 nm) and the LiF cladding (n = 1.4 at 450 nm, according to luxpop) means that a large number of modes will be guided, and that the field associated with most modes will not penetrate far into the cladding.
- If the LiF particles are embedded in a cladding with a refractive index closer to that of the core, this will improve the modal penetration into the cladding; however, note that the relatively large LiF particles will have a significant impact on the overall cladding refractive index if they are positioned near the core in high density.
- Using metal as the outermost cladding to try to improve modal overlap with the scintillator is a potentially risky strategy, as metals are typically absorbing at optical wavelengths. Having metal near the core will increase the optical loss of the fiber. Having metal far from the core will have little impact, except perhaps to guide additional modes which would otherwise be leaky, but these modes will experience loss in the metal.
- It may make the most sense from a purely optical standpoint to choose ZnS:Ag as the inner cladding for maximum overlap with the core-guided optical mode, and ^{6}LiF as the outer cladding. ZnS has a higher refractive index (2.5 according to luxpop) so it should encourage modal penetration into the cladding.
- However, it may be possible to use ZnS:Ag as the outer cladding and still get sufficient modal overlap, assuming the ^{6}LiF inner cladding isn't too thick.
- An alternative strategy would be to anti-guide the core by using a material with lower refractive index than the LiF cladding.
- If larger fibers with high index contrast are desired, a ray-tracing analysis may be more appropriate.

Sample Results

Figure 2 shows two calculated mode patterns for a 2-layer waveguide with a silica core and a LiF cladding. Most of the modes have little penetration into the cladding for this index contrast. This illustrates the importance of placing the scintillator material near to the fiber core for strong coupling of the scintillation light into the guided mode to occur in this configuration.

Neutron Detector Modeling

Sample neutron detector configurations have been created in MCNPX. These sample configurations followed a simple design where an inert fiber optic core of borosilicate glass was clad in ZnS:Ag coated ^{6}LiF grains. The lithium-6 enrichment was assumed to be 95%. This configuration can be seen in Figure **3**. A second configuration where a lower index of refraction coating was applied over the ZnS:Ag coated LiF layer. This would be done to improve the light transmission down the fiber. This material was selected to be PMMA. This configuration can be seen in Figure 4.

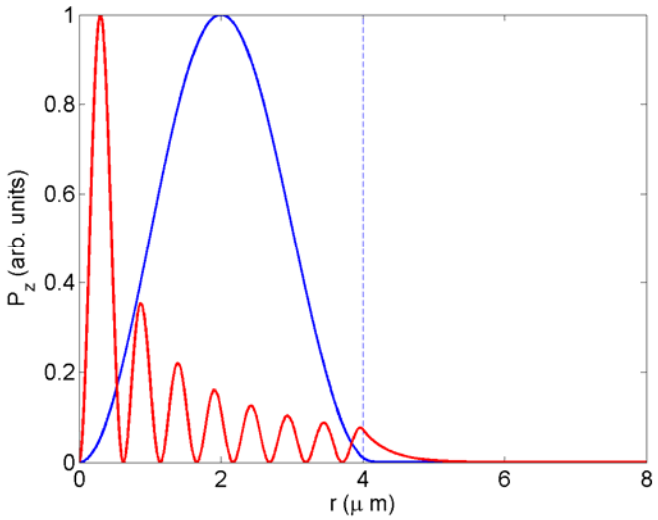

Figure 2. The z-component of the Poynting vector (time average power per area propagating in the z-direction) of a low-order (blue) and a higher-order (red) TE guided mode in the waveguide. The boundary between core and cladding is indicated with a dashed line. Note the relatively small penetration of the mode into the cladding.

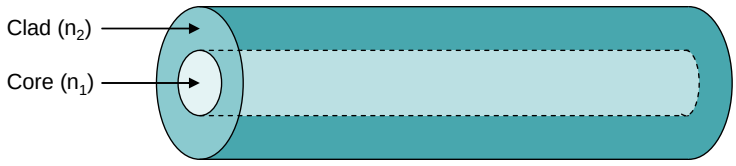

Figure 3. Sketch of a typical optical fiber composed of a core material covered by a clad material. $n_1$and n_2 are refractive indices.

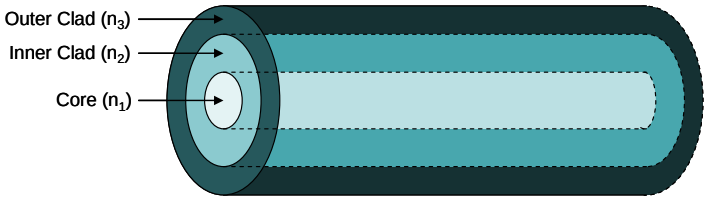

Figure 4. Sketch of a double clad optical fiber. n_1, n_2 and n_3 are refractive indices.

Simple optimization of the ZnS:Ag layer has found that thicknesses need only be 5 microns to fully collect the energy of the recoiling alpha particle. To fully range out the recoil tritium, a thickness of 10 microns is needed to accommodate variations in the source origin. Plots of the energy deposition

curves are shown in Figure 5. Shown in Figure 6 is the two dimensional particle trajectory plot for alphas produced in the ^{6}Li(n,α) reaction. As seen in these figures, thicknesses above 10 microns is not needed to fully stop the charged particles. Using this number, we will scope chemical vapor deposition methods for applying up to a 10 um coating over LiF grains.

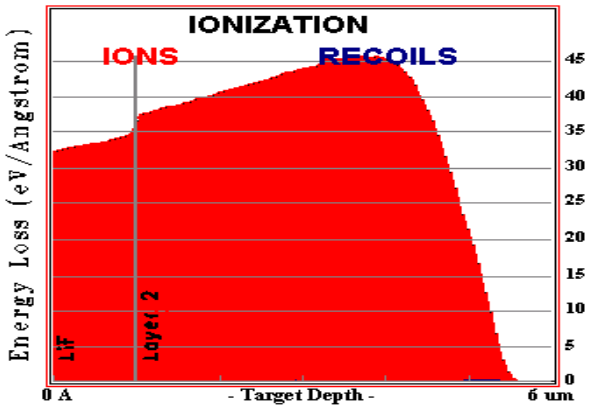

Figure 5. Energy loss as a function of depth in the LiF and ZnS:Ag layers for recoiling alpha particles.

Neutron Efficiency Modeling

To determine a sample detector configuration's neutron detection efficiency, several configurations were modeled on a macroscopic scale. Packaged in varying diameters of polyethylene shielding, neutron detection efficiencies were carried out in MCNP5. Polyethylene rods were assumed to be bored out with a fiber bundle modeled as a homogenized mix of borosilicate glass, ZnS:Ag, ^{6}LiF, and Polymethylmerthacrylate (PMMA). This will be modified to consist of actual single fibers when more data becomes available on the singular fibers. An efficiency versus energy as a function of polyethylene radius is now being computed. Images of the MCNP model can be seen in Figure 7 and Figure 8. It is seen that the fibers will exhibit an increasing response for the higher energy neutrons with larger radii.

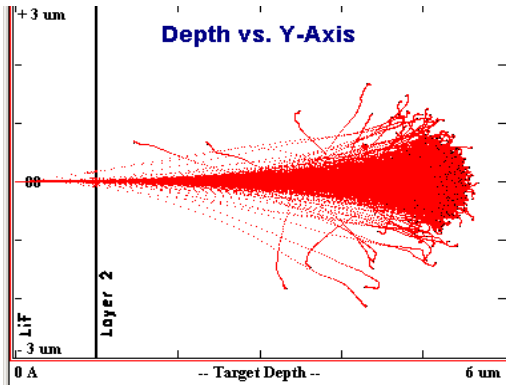

Figure 6. Alpha particle trajectories created in a 3 um thickness.

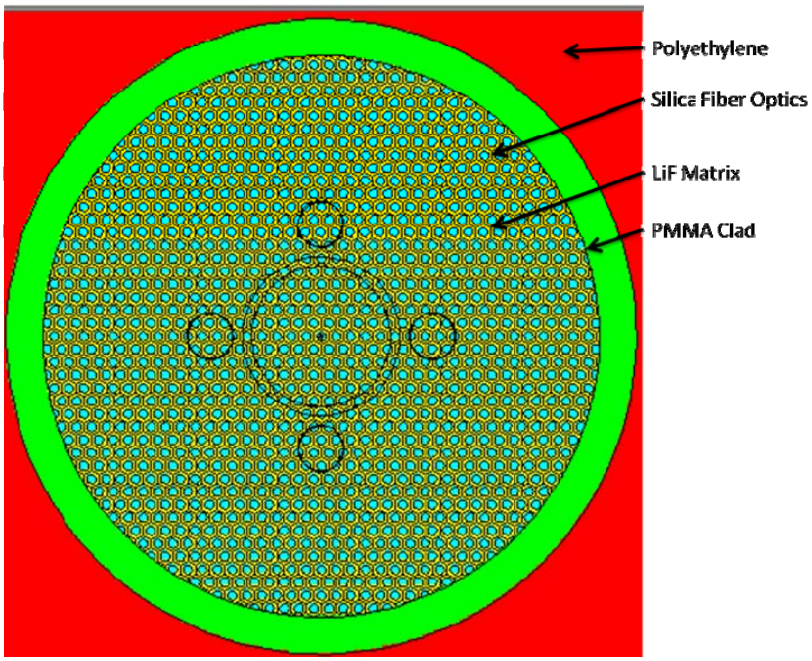

Figure 7. MCNP model of macroscopic fiber bundle including LiF matrix silica fibers a PMMA cladding and a polyethylene moderator.

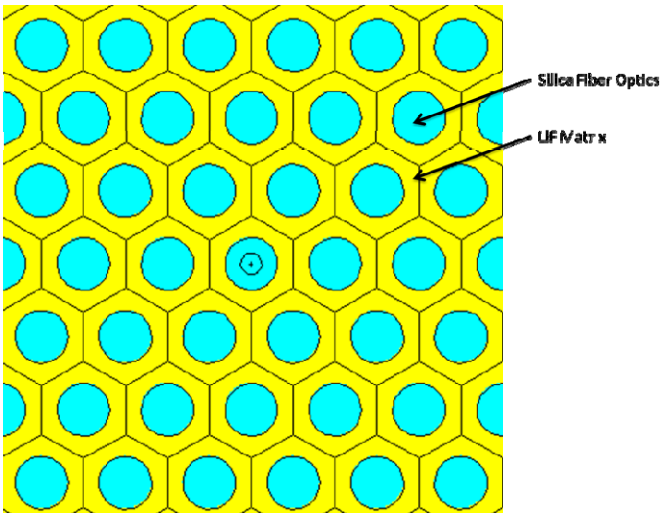

Figure 8. Microscopic view of silica fibers in LiF matrix MCNP model.

ZnS:Ag Coating Techniques

Several different coating techniques have been investigated as potential routes to coating the LiF grains. One potential method is through chemical vapor deposition (CVD). Using CVD, the grains are introduced into a vacuum chamber along with two pure samples of zinc and sulfur. Atmospheric air is removed and an inert fill gas is introduced at a very low pressure. The zinc and sulfur sources are heated to the gaseous phase and allowed to deposit on the grains.[1] A second is atomic layer deposition (ALD). In ALD, the growth process is more controlled. Single atomic layers are deposited one at a time by controlling the deposition rate of the first zinc precursor, and then introducing a reactive gas to deposit the sulfur. In Figure 9 an image depicting the ALD process is shown with the ALD growth of ZnS from $ZnCl_2$ and H_2S being illustrated, namely:

- $ZnCl_2$(g) adsorbs into the surface nucleating growth.
- Nitrogen is used as a purge gas to sweep the excess $ZnCl_2$(g) from the surface.
- H_2S(g) reacts with $ZnCl_2$ forming ZnS(s) and HCl(g) on the surface.
- Nitrogen sweeps the excess) H_2S(g), $ZnCl_2$, ZnS(s) and HCl(g) from the surface.
- At this point, a single atomic layer of ZnS has been deposited.

This process is repeated for as many layers or thicknesses as the operator wants. In this technique, the reactants are sequentially transported to the substrate as pulses, such that only one is supplied to the substrate at a time. Each pulse is followed by a "dead time," which may involve an inert or reactive gas purge (sometimes H_2 is used) before the other reactant is pulsed. These pulses are either neutral molecules or atoms, delivered as chopped beams in the case of high or ultrahigh vacuum systems, or as switched vapor streams in the case of gas flow ALD.

The films that result from ALD are high quality and conformal, even for low length scale structures. The technique has been used to successfully grow complex multi-layered structures, such as layered Ta_xAl_yO film [2] Al_2O_3 ultrathin coatings on BN particles, [3] and high aspect ratio $Hf_xAl_yO_2$ coatings. The latter structures are the important to this study because they show that the necessary coating characteristics are achievable. ALD is able to grow very thin (nano-sized) films that can remain conformal even on abrupt features such as in the 90 degree bend shown in the TEM images in Figure 10.

Radiation Testing

The Georgia Tech NRE program has extensive experience in performing neutron spectral and dosimetry measurements as well as an extensive computational radiation transport capability. Reference neutron fields have been created for the calibration and testing of instruments as well as for use in measurement technique development. Many of these reference neutron fields are based on a ^{252}Cf neutron source (ISO 8529 reference field) and its modification by a 30 cm diameter, cadmium-covered D_2O sphere (ISO 8529 reference field); a 30 cm thick iron spherical shell, a 30 cm diameter polyethylene sphere, a 16 cm thick lead spherical shell, and a 9 cm thick tantalum spherical shell. Complementing this Cf-252 spontaneous fission source, is a 54 Ci AmBe neutron source (ISO 8529 reference field) is available to test instrument response in higher energy fields. The AmBe source can also be inserted in the iron, tantalum, and polyethylene spherical shells described above. In addition, a pulsed neutron generator is currently being repaired which can produce 2 MeV (DD) or 14 MeV (DT) neutron fields.

Tests will be conducted once viable fiber samples are made available. The PIs also have access to visible light spectrometers and many other photon detection systems to quantify the light yields from these scintillators.

.

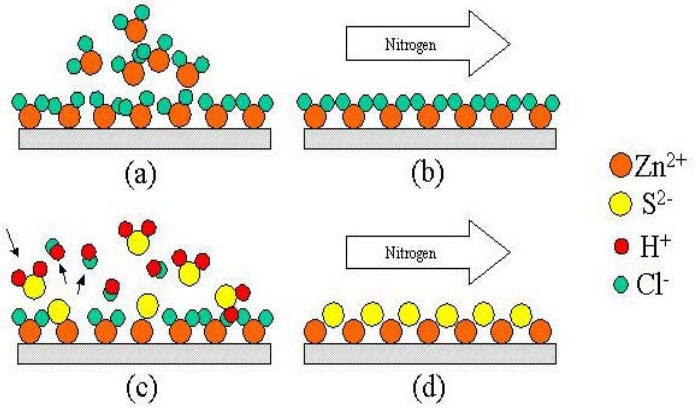

Figure 9. Growth process of ZnS utilizing the ALD process.

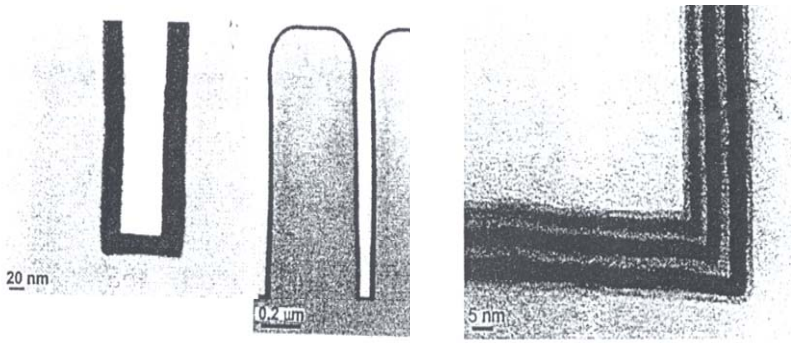

Figure 10. TEM images of $Hf_XAl_YO_2$ composite structure. At right, detail of corner.

References

1. F. Zhenyi et al. "CVD Growth of Bulk Polycrystalline ZnS and its Optical Properties" Journal of Crystal Growth Vol 237-239 , 1707-1710 (2002).
2. H. Kattelus, M. Ylilammi, J. Saarilahti, J. Antson, S. Lindfors, Thin Solid Films, 225, 296 (1993).
3. J. D. Ferguson, A. W. Weimer, S. M. George, Thin Solid Films, 371, 95 (2000).